ACS MATERIALS LETTERS

www.acsmaterialsletters.org

LETTER

A Bioinspired, Durable, and Nondisposable Transparent Graphene Skin Electrode for Electrophysiological Signal Detection

Jiakang Qiu,[▽] Tianhao Yu,[▽] Weifeng Zhang, Zihan Zhao, Yan Zhang, Guo Ye, Yan Zhao, Xiaojia Du, Xu Liu, Lu Yang, Lijuan Zhang, Shuyan Qi, Qishuo Tan, Xinyu Guo, Guanmeng Li, Shaoshi Guo, Huiyuan Sun, Di Wei, and Nan Liu*

Cite This: *ACS Materials Lett.* 2020, 2, 999–1007

Read Online

ACCESS | Metrics & More | Article Recommendations | Supporting Information

ABSTRACT: **Graphene, with its properties of intrinsic flexibility, reliable electrical performance, and high chemical stability, is highly desirable as bioelectrodes for detecting electrophysiological signals. However, its mechanical properties limit its application to a great extent—energy dissipation mechanisms are not provided by the carbon network for external strain and it easily cracks. Herein, inspired by the very structure of the avian nest, we report a durable and nondisposable transparent graphene skin electrode for detecting electrophysiological signals, which was fabricated by semi-embedding highly graphitized electrospun fiber/monolayer graphene (GFG) into soft elastomer. Because of the semi-embedded structure and strong interaction between annealed electrospun fiber and graphene through graphitization, as-fabricated conductive film demonstrated high conductivity and transparency (~150 Ω/□ at 83% transmittance), as well as a stable electrical performance under mechanical vibrations (strain, peel-off, stir, etc.). It can be used to reliably collect vital biometric signals, such as electrocardiogram (ECG), surface electromyogram (sEMG), and electroencephalogram (EEG). Furthermore, the semi-embedded GFG in the elastomer demonstrated excellent washability (rinsing/stirring in water) and repeatability (~10 repeats) with high signal-to-noise ratio (up to 30 dB) while detecting sEMG. This is the first report of durable and transparent graphene skin electrode for biometric signals detection, revealing potential opportunities in wearable healthcare applications.**

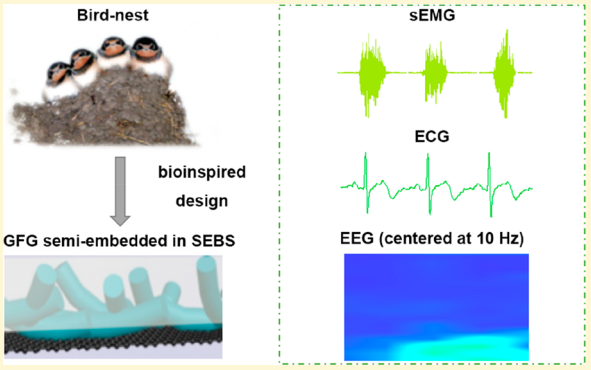

Unlike conventional medical devices, skin-like electronic[1,2] systems attached onto the surface of the skin provide a platform technology for diverse physical and electrophysiological signal acquisition,[3,4] energy storage/transmission and signal processing/transduction, etc. For these wearable electronics, accuracy without collateral damage to the skin is the primary consideration for healthcare applications.[2] This is because stable monitoring of steady-state visually evoked potentials (SSVEP) to control robotics,[5,6] epilepsy and glaucoma diagnosis,[7] or neonatal monitoring; all require accurate and robust electrosphysiological signal detection. Currently, hydrogel-based "wet" Ag/AgCl electrodes are commonly applied in electrophysiological signal detection, where conductive gel or paste is used to reduce the impedance as well as making conformal contacts between the human skin and the electrodes.[8] While the commercialized electrodes provide adequate signal quality,[8,9] their disadvantages in long-term use and irritation to the skin still remains intractable.

Regarding these disadvantages, on-skin sensors made by precious metal have been developed for use as electrocardiograms (ECGs),[10,11] surface electromyograms (sEMGs),[12,13] and electroencephalograms (EEGs).[13,14] Among these on-skin sensors, gold (Au) was chosen most often as the sensing material for its biocompatibility and ductility.[15−20] For instance, a 300-nm thin film made by Au and parylene was reported to be self-adhesive to biological surfaces, but its ultrathin nature was not easy to handle for daily use.[9] Paper or medical tapes were used to handle ultrathin film that contained

Received: May 14, 2020
Accepted: July 16, 2020
Published: July 16, 2020

https://dx.doi.org/10.1021/acsmaterialslett.0c00203
ACS Materials Lett. 2020, 2, 999–1007

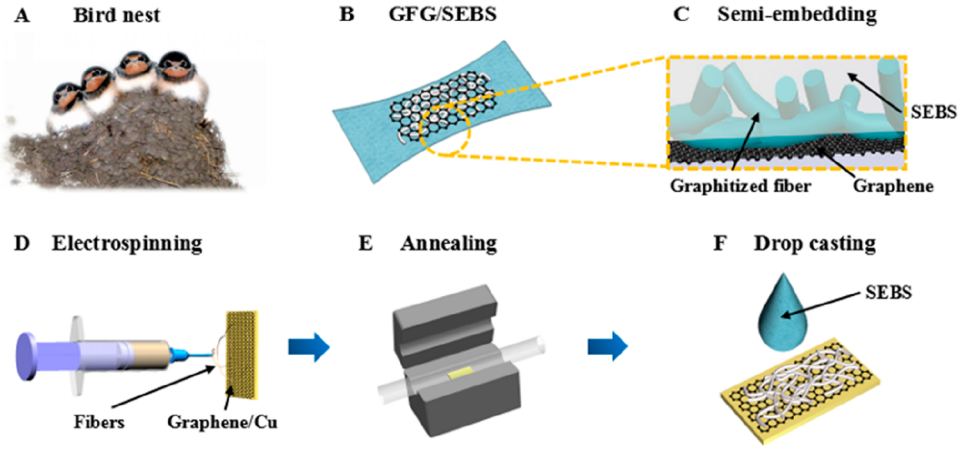

Figure 1. Schematics of fabrication of semi-embedded graphitized electrospun fiber/monolayer graphene (GFG) as nondisposable graphene-based skin-electrodes. (a) Schematic of a bird's nest, which was mechanically reinforced by tightly connected polysaccharide. (b, c) Schematic of GFG film semi-embedded in SEBS elastomer with a cross-sectional view (panel (c)). (d–f) Schematic fabrication process of GFG. In panel (d), the polymer fibers were electrostatically spun on the surface of graphene grown on Cu foil by CVD. In panel (e), the fibers/graphene/Cu foil were annealed under an atmosphere of argon. In panel (f), SEBS solution was dropcast on their surface and semi-embedded into the entire structure of fibers/graphene/Cu foil. After the copper was etched away, semi-embedded GFG film was formed as illustrated in panels (b) and (c).

Au-coated polyethylene terephthalate (PET) onto skin.[21] In addition, gold is expensive and visually visible, making it unsuitable for imperceptible sensing. For example, when making Au into a nanomesh structure to enable the on-skin sensor to be inflammation-free, gas-permeable, and stretchable, the cost and visibility of gold, together with expensive and time-consuming vacuum deposition processes, greatly limit its accessibility.[22] Considering the biocompatibility and ductility, metals other than Au were rarely reported to be applied in skin-electronic system for electrophysiological signal detection.[23,24] Overall, it is eager to search for inexpensive, lightweight, transparent, and robust conductive materials to realize long-term and repeated monitoring of electrophysiological signals on human skin.

Graphene, as a one-atom-thin conductive material, is biocompatible, optically transparent, and electrochemically stable.[25−27] Among all the sources of graphene, graphene grown using chemical vapor deposition (CVD) methods is regarded to provide the best quality, in terms of conductivity and transparency. To enable graphene to be an appropriate material for on-skin electrophysiological sensors,[28] electro-mechanical stability and robustness of graphene are two challenges to overcome first. A transparent graphene e-tattoo held by 3M Tegaderm tape was reported to be able to maintain conductivity under high strain and detect electrophysiological signals accurately.[8] However, such e-tattoos are subjected to complex manufacturing processes, as well as the fragile nature of one-atom-thick graphene layers. Recently, Liu et al.[29] demonstrated that electrostatically spun polyacrylonitrile nanofibers on the graphene film can enhance the electrical and mechanical properties of graphene electrodes, but their performance as skin electrodes for electrophysiological signal detection has not been investigated. Since skin electrodes will be exposed to repeated and prolonged mechanical stresses[30] (friction force, tensile and compressed strain etc.), a robust and durable on-skin sensor is urgently needed, to reliably measure vital electrophysiological signs, with regard to the patients under different scenarios.

A bird's nest is a natural structure with marvelous firmness. Many studies have attempted to characterize and understand its construction.[31] It was reported that polysaccharide, which is a large molecule that consists of many sugar molecules bonded together, when excreted by a bird, can enhance the mechanical behavior of the mud-based nest.[32] Inspired by the solidification process of filiform saliva, we reported the fabrication of a robust and nondisposable graphene-based conductive film for repeated use in electrophysiological signal detection. The as-prepared conductive film consisted of annealed phenolic resin (PR) fibers electrospun onto CVD graphene, and then semi-embedded into a styrene−ethylene−butylene−styrene (SEBS) elastomer. High-temperature annealing enabled electrospun polymer fibers to strongly interact with monolayer graphene, which, together with a semi-embedding process, mimicked the formation of a bird's nest. The film demonstrated a low sheet resistance with stable electrical performance under mechanical vibrations (strain, peel-off, stir, etc.). Because of the mechanical and electrical integrity of the network, the graphene-based conductive film can be applied on skin to detect vital bio-signals and it offered the abilities of being washable and reusable. This is the first demonstration of robust and nondisposable graphene-based skin electrodes, suggesting a proper strategy toward high-performance wearable healthcare monitors.

■ RESULTS AND DISCUSSION

To bear natural loads of birds and eggs, a bird's nest is built by means of joint materials to retain physical integrity. Applying materials that inherently stick with each other and surrounding mud is proved to be one way to enhance mechanical behavior (see Figure 1a). Inspired by this principle of a bird's nest, we designed a joint carbon network semi-embedded into elastomer to enable a robust and nondisposable skin electrode for detection of electrophysiological signals (see Figures 1b and 1c). The fabrication process is illustrated in Figures 1d–f. Polymer nanofibers were first electrospun on the surface of monolayer graphene film (Figure 1d), which was synthesized on copper foil by CVD method. Electrospun polymer solution

https://dx.doi.org/10.1021/acsmaterialslett.0c00203
ACS Materials Lett. 2020, 2, 999−1007

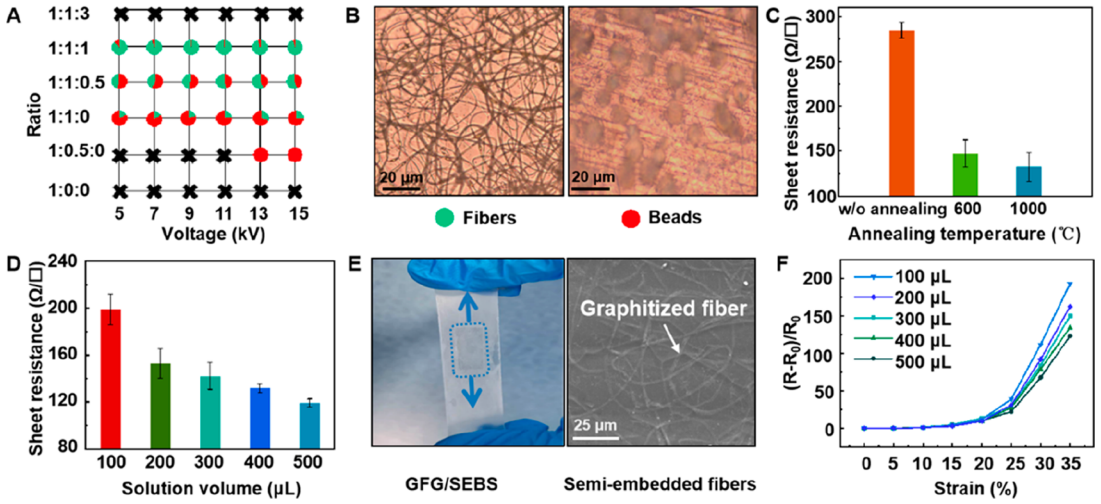

Figure 2. Fabrication and characterization of the semi-embedded GFG. (a) Statistics of the specific morphologies (fibers and beads) of the electrospun fibers prepared under different conditions (component ratio of $CuCl_2$, SEBS, and PR versus electrospun voltage). (b) Representative optical images of fiberlike and beadlike electrospun fibers on graphene/Cu foil. (c) Sheet resistance of electrospun fiber/graphene annealing at 600 °C (green), 1000 °C (blue), and without (red) annealing. (d) Sheet resistance of GFG as a function of volume of electrospun polymer solution (annealed at 600 °C). (e) Photograph (left) and SEM image (right) of the semi-embedded GFG. (f) Resistance change of the semi-embedded GFG, as a function of uniaxial stretching strains.

contained three components: copper chloride ($CuCl_2$), SEBS, and phenolic resin (PR), all dissolved in tetrahydrofuran (THF). The fibers together with graphene on copper foil were annealed under an atmosphere of argon, going through carbonization reactions at high temperature (Figure 1e). As a result, the interlaced fibers attached tightly onto the graphene surface by $\pi-\pi$ interaction.[33] The interaction between phenol side groups and metal cations helped to promote the growth of crystalline graphene structure. In addition, the benzene moieties in the polymer may facilitate the formation of highly crystalline graphene.[34] Laser scribing on polyimide, wood, and textiles is another method to obtain crystalline graphene structure, which has an advantage in patterning.[35−37] It is also applicable here to replace graphitized electrospun polymer (GFG); however, precursors with rich lignin are needed. SEBS solution (SEBS (MW ≈ 118 000) in toluene, 120 mg/mL) was dropcasted and embedded the entire graphitized nanofibers/graphene/Cu foil (Figure 1f). After toluene solvent was evaporated, underlying copper foil was etched off in ammonium persulfate solution (Figure S1 in the Supporting Information). The as-prepared electrode had a similar structure as a bird's nest, with strongly bonded carbon network semi-embedded in SEBS elastomer (Figure 1a and b). By this design, we hypothesized that this electrodes that can work as robust skin electrodes for detection of electrophysiological signals.

The morphology of the electrospun fibers would directly affect the electrical conductivity of the corresponding GFG. In addition, it could be controlled by adjusting the viscosity of the polymer solution and the electrospinning voltage. Statistics of the specific morphologies, as a function of viscosity of the electrospinning solution versus voltage, is shown in Figure 2a, and optical images of the electrospun polymer fibers prepared under different conditions are shown in Figure 2b. Generally, the polymer fibers used to constitute an electrode were required to be without beads, which, in this work, were electrospun by regulating the ratio of the weight of three components and voltage as 1:1:1 and 9 kV, respectively. Meanwhile, metal salt affects the viscosity and electrical conductivity of the polymer solution.[38] A modification of the polymeric electrospun nanofiber mats can be achieved by addition of inorganic metal salt to the polymer solution. Utilizing of $CuCl_2$ had positive impact on the morphology of the fiber in this work. After annealing, higher temperature causes serious shrinkage to the fiber, because of volatilization of phenolic resin during graphitization (see Figure S2).

High-temperature graphitization of the electrospun fiber mesh on graphene could contribute to the electrical performance of the film. The sheet resistance of electrospun fiber/graphene before annealing was near 275 Ω/□ and was in accordance with a graphene monolayer.[33] Figure 2c demonstrated that an annealing temperature of 600 °C provided better conductivities with sheet resistances of ∼150 Ω/□, which is almost 50% less, compared to that before annealing, which may be ascribed to that annealed fiber network provide additional pathways for electron transportation. Figure S3 in the Supporting Information shows the X-ray photoelectron spectroscopy (XPS) spectra of GFG film annealed under different temperatures. As the temperature rises, the fibers are gradually carbonized and graphitized. It was revealed by Raman spectra that the increasing annealing temperature also led to a higher degree of graphitization in nanofibers as the ratio of I_D/I_G decreased (see Figure S3). However, the progressive increasing temperature no further ended with a distinct decrease in resistance. Thus, 600 °C was chosen for the annealing process. After annealing, since fibers tightly adhered to the graphene (Figure 2e), the integrity of GFG film was preserved.

Fiber density is another crucial parameter that affects the electrical conductivity of the GFG film. When the volume of the solution was increased to 200 μL, more-effective conductive channels were formed, which made the resistance lower (Figure 2d). Uniaxial tensile tests were performed to identify the strain-conductivity behavior of thus-fabricated electrode. It remained electrically conductive up to a strain of 35% (Figure 2f), which conformed with the stretchability of the human skin.[39] The strain-electrical behavior improved with the increasing densities of graphitized-electrospun fibers. In

https://dx.doi.org/10.1021/acsmaterialslett.0c00203
ACS Materials Lett. 2020, 2, 999−1007

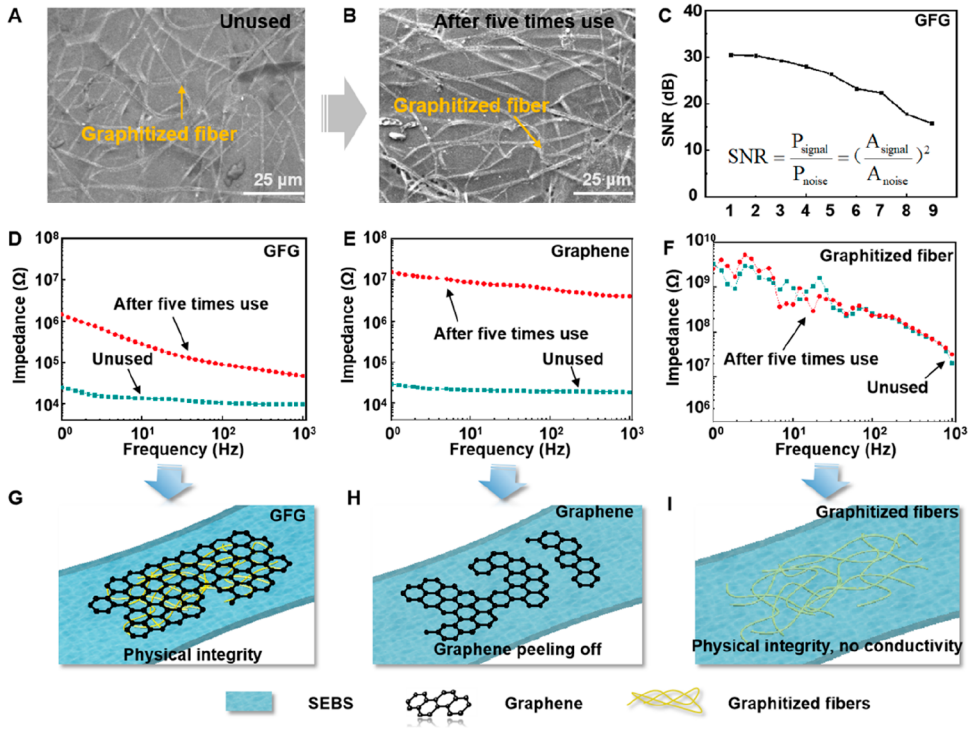

Figure 3. Understanding of repeated-use performance of GFG/SEBS. (a, b) Morphology comparison of GFG/SEBS before use (panel (a)) and after being used for five times (panel (b)). (c) SNR of sEMG detected by GFG/SEBS versus number of uses. (d–f) Impedance magnitude versus frequency of GFG/SEBS (panel (d)), graphene/SEBS (panel (e)), annealed fiber/SEBS (panel (f)), and their changes after five cycles of attaching–detaching-to-skin. (g–i) Schematic drawings of microstructures of GFG/SEBS (panel (g)), graphene/SEBS (panel (h)), and annealed fibers/SEBS (panel (i)) after repeated use on skin.

pure graphene, once a slit formed, the stress concentrated in a tip of the slit, leading to crack propagation and damage of the electrode.[40] In contrast, for semi-embedded fibers in a soft substrate, the substrate dissipated the stress and allowed crack elsewhere to rupture. This mechanism ensured that the semi-embedded GFG would still be conductive, even when stretched to strains up to 35%, which was significantly greater than what the monolayer graphene/SEBS can withstand (6%).[41] When the electrospinning polymer solution increased to more than 200 μL, the sheet resistances and resistance changes versus strain of GFG/SEBS electrode showed slight differences, compared with the 200 μL (Figure 2d). Considering the cost and transparency, we selected a volume of 200 μL electrospinning polymer precursor solution for fabricating durable electrodes, showing a transparency of 83% at λ = 550 nm (Figure S4 in the Supporting Information) and low sheet resistance of ~150 Ω/□.

To understand the repeated-use performance of GFG/SEBS, we performed peel-off tests and compared the changes of morphology and electrical impedance. The scanning electron microscopy (SEM) images (see Figures 3a and 3b) showed a nonobvious morphology change of the film surface before and after use. After five attaching–detaching-to-skin tests, carbonized fibers were basically retained, while monolayer graphene was difficult to be distinguished on SEBS both before and after use. For each attaching–detaching use, it is ~10 min, so five uses requires ~1 h. We hypothesized that carbonized fibers formed a homogenous combination with graphene during annealing and acted as conductive network semi-embedded in SEBS that maintained electrical conductivity in peeling off, increasing the chance of the electrode collecting human skin surface bioelectricities (Figure 3g). Also, the carbon soldering joints prevented the graphene from being peeled off and contributed to more conductive channels (Figure S5 in the Supporting Information). As a result, SNR of sEMG signal detected by GFG/SEBS slowly decreased and still maintained above 20 after being used seven times (see Figure 3c). The interface impedance can display the ability to detect the physiological signal of electrode. We measured and compared the electrochemical impedance spectra (EIS) of the graphene electrode, GFG, and annealed fibers on SEBS by using an electrochemical workstation. Although the impedance of GFG/SEBS showed an increase after five attaching–detaching-to-skin cycles, the impedance change was much smaller than that of graphene/SEBS (see Figures 3d and 3e). The improved interfacial property will be beneficial to multiple measurements, even combined with clothing to withstand multiple washes and other wear. Mechanical damage of washing mainly occurs when the electrode gets rid of water, because of surface tension, causing reduction of conductive channels (see the discussion of washing and usage on the durability of semi-embedded GFG in SEBS; see Figure S6 in the Supporting Information). When pure graphene on SEBS was washed or used on skin a few times, its function as an electrode was greatly affected. Because of the poor adhesion of graphene to flexible SEBS substrate, the lesser remaining quantity of graphene after washing led to a sudden impedance increase and an improper conduction (Figure 3h versus 3g). As for the fiber without graphene, it exhibited extremely high impedance both before and after use, possibly because the annealed fibers are completely embedded in the flexible substrate, there are not enough joint junctions, and they are not conductive (Figure 3f). Overall, the basically unchanged morphology and modest impedance of GFG/SEBS after being

https://dx.doi.org/10.1021/acsmaterialslett.0c00203
ACS Materials Lett. 2020, 2, 999–1007

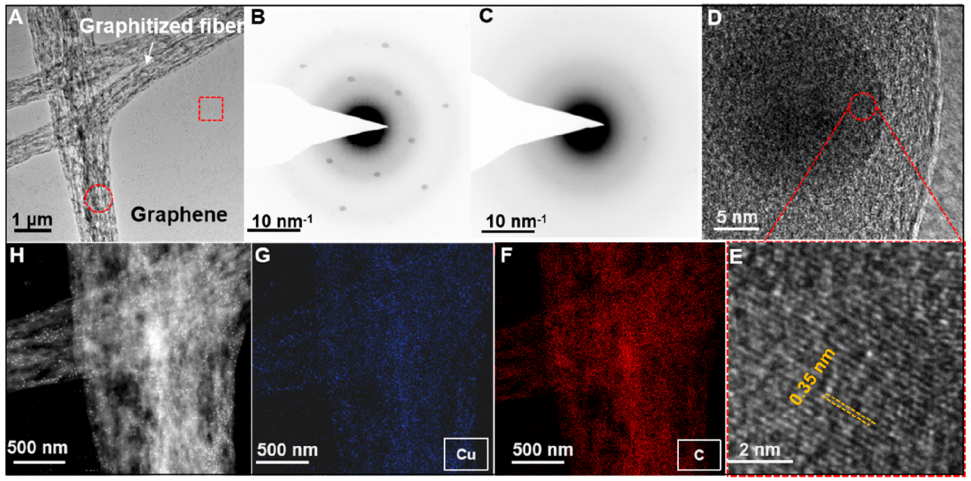

Figure 4. Structure characterizations of GFG. (a) A low-resolution TEM image of suspended GFG. (b, c) SAED patterns of the graphene area (panel (b)) and GFG (panel (c)) area circled in panel (a). Scale bar = 10 nm^{-1}. (d, e) High-resolution TEM observations of GFG. Panel (e) shows an expanded view of the TEM image shown in panel (d), showing a high degree of graphitization with lattice spacing of 0.35 nm. (f–h) TEM observation and corresponding EDS mapping analysis of a junction formed in GFG. Panels (f) and (g) show the EDS mapping of elemental carbon and copper, respectively.

used on skin a few times, reflected the stability and high mechanical durability of this structure, which is suitable as a durable and nondisposable skin electrode.

Transmission electron microscopy (TEM) was used to characterize the microstructure of GFG (Figure 4a) with a graphitizing temperature of 600 °C. The diameter of graphitized-electrospun fibers is in the range of 0.5−1.5 μm. Selected-area electron diffraction (SAED) image of graphene region outlined a single set of dots with hexagonal symmetry (Figure 4b), while that of GFG showed a diffraction circle exhibiting the polycrystalline nature of annealed-electrospun fiber on graphene (Figure 4c). To evaluate the graphitic domain sizes and correlate them with elemental copper in the polymer, we performed high-resolution transmission electron microscopy (TEM) observations. Figure 4d show the atomic-resolution image, and the magnified pattern in Figure 4e demonstrate a great degree of graphitization. The observable lattice fringe spacing was estimated to be ∼0.35 nm, which closely matched the interplanar spacing of graphene.[42] The fibers could attach tightly onto the graphene surface by the welding of carbonization. In addition, this is consistent with our XPS study, which confirmed that the polymer containing elemental copper will result in a higher degree of graphitization. The obvious fusion of fiber junctions suggested a strong bonding in the junctions (Figure 4h). The corresponding energy-dispersive spectroscopy (EDS) mapping images were further collected (see Figures 4f and 4g). From the high-angle annular dark field (HAADF) image, it can be found that elemental copper were uniformly located in the fiber corresponding to areas with a high degree of graphitization. The presence of copper improved the degree of graphitization and thus would promote the conductivity of the fiber. Similar to an avian nest, it is likely that these well-carbonized welding points could contribute to the morphological and mechanical integrity of the film.

To investigate the potential of semi-embedded GFG in SEBS as a robust and nondisposable skin electrode, we used it to detect sEMG signals and recycled the usage multiple times. Safety issues of this skin electrode, with regard to Cu^{2+}, is discussed in the Supporting Information. We mounted the electrode on a volunteer's forearm for signal recording (Figure 5b). A dynamometer was applied to ensure an identical force for each test, and infrared imaging (Figure 5f) demonstrated that wearing the GFG/SEBS brought a very small level of heat accumulation to the skin. The amplitude of the obtained signals was comparable to those obtained by gel electrodes with a slight baseline noise. In addition, the SNR was as high as 30 dB and it can be used up to nine times (see Figure 5d, as well as Figure S7 in the Supporting Information). More attach−remove actions would damage its conductivity, because of the slight crack of graphene, but it can maintain its structure and it can be reusable within a reasonable period. In contrast, graphene on SEBS without GFG structure showed a sharp increase in baseline noise. It was seriously damaged by performing peel-off tests five times, and a significant decrease in signal quality was observed. Furthermore, we compared the sEMG detection of GFG/SEBS and graphene/SEBS after rinsing in water by using a magnetic stirrer (250 rpm for 15 min). The measured signal from GFG/SEBS was almost the same after five uses, while graphene/SEBS failed in the detection after only one use (Figure 5e). Such excellent durability can be contributed to the combination of the graphene coupling with annealed fibers semi-embedded in polymer (see Figure S5). To further enhance the durability of GFG, dense graphitized electrospun fibers soldering on multilayer graphene are required to be semi-embedded in SEBS. However, the involvement of more-conductive channels semi-embedded in the soft matrix will compromise electrode transmittance and fabrication cost. Benefit from the mechanical-integrity-reinforced and electrical-conduction-enhanced properties, GFG/SEBS is appropriate for on-skin signal recording and can be used cyclically.

GFG/SEBS can also monitor the electrophysiological process related to the activities of the heart (ECG) and the brain (EEG). By using the Einthoven triangle principle,[43] three GFG/SEBS were placed on right arm, left arm, and left leg (see Figures 5g and 5h). In Figure 5i, several vital signals (P, QRS complex, and T) are successfully recorded by GFG/SEBS. The reference test for Ag/AgCl was done separately but in exactly the same positions. Typical waves were clearly recognizable

https://dx.doi.org/10.1021/acsmaterialslett.0c00203
ACS Materials Lett. 2020, 2, 999−1007

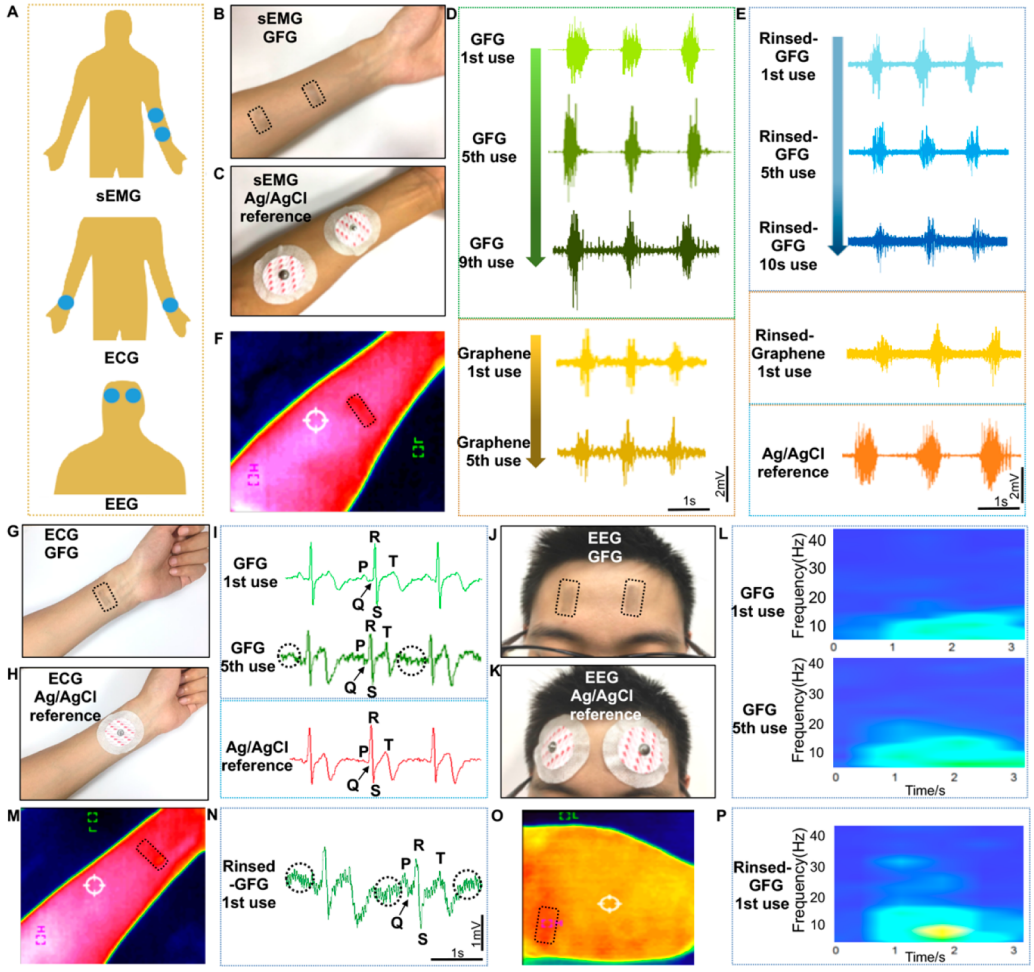

Figure 5. GFG/SEBS as a robust and nondisposable skin electrode for sEMG, ECG, and EEG detection. (a) Schematics of the electrodes on body. (b, c) Photographs of wearing the GFG/SEBS and the Ag/AgCl electrodes to detect sEMG, respectively. (d) sEMG measured by GFG/SEBS for the first use, the fifth use, and the ninth use, respectively, and sEMG measured by graphene for the first use and the fifth use, respectively. (e) sEMG measured by GFG/SEBS after rinsing in water (250 rpm for 15 min) for the first use, the fifth use, and the tenth use, and graphene/SEBS after rinsing in a flume. sEMG measured by Ag/AgCl electrodes as reference. (f) Infrared image of the GFG/SEBS on a forearm. (g, h) Photographs of wearing the GFG/SEBS (panel (g)) and the Ag/AgCl electrode (panel (h)), as the ECG sensor. (i) ECG recorded from the wrist of a volunteer by GFG/SEBS (top), and after being used five times (middle), and Ag/AgCl electrodes (bottom). Magnified ECG signal indicated clear P-wave, QRS complex, and T-wave. (j, k) Photographs of wearing the GFG/SEBS (panel (j)) and Ag/AgCl electrodes (panel (k)) as the EEG sensor. (l) EEG recorded from the forehead of a volunteer by GFG/SEBS (top), and after five cycles of attaching-detaching (bottom). Alpha rhythm centered at ~10 Hz. (m) Infrared image of the GFG/SEBS on the forearm. (n) ECG measured by GFG/SEBS after rinsing in water. (o) Infrared image of the GFG/SEBS on the forehead. (p) EEG measured by GFG/SEBS after rinsing in a flume.

received by both electrodes, and characteristic peaks can be identified in both waveforms as well. Even after rinsing in a flume, GFG/SEBS can still reveal the QRS morphological features without significant distortion, giving an acceptable ECG signal (Figure 5n).

EEG recording is a more challenging test for biopotential electrodes, because of the low signal amplitudes in the microvolt (μV) range. Two GFGs were used to detect alpha wave activity from the forehead positions, as shown in Figure 5k, and a reference was placed near the earlobe. A volunteer was in a relaxed and stationary status with their eyes closed. The recordings in fast Fourier transform (Figure 5l) indicate a visible 10 Hz domain, which is characteristic for alpha waves. And after the eyes were opened, the domain disappeared. During a half an hour of measurement, the volunteer did not experience any discomfort with the GFGs attached, and this represents an advantage over existing commercial electrodes. Again, infrared images showed that wearing the GFG/SEBS brought no extra heating to the skin (Figures 5m and 5o), exhibiting reasonable comfortability. After attaching−detaching to skin several times and being rinsed in a flume, GFG/SEBS can still detect clear alpha wave activity (see Figures 5l and 5p), indicating that it can work as a nondisposable skin electrode for electrophysiological signal detection.

We have designed a graphene-based electrode with stable structure for repeated use in vital electrophysiological signal detection. This electrode was fabricated by mimicking a bird's nest, composed of graphitizing electrospun fibers on graphene and semi-embedding them in soft elastomer such as SEBS. Because of the welding joints formed by graphitization and semi-embedded structure similar to a bird's nest, GFG/SEBS exhibited excellent morphological and mechanical integrity, maintaining conductive in a long-term use on skin even under mechanical vibration (peel-off, strain, rinsing, etc.). This

https://dx.doi.org/10.1021/acsmaterialslett.0c00203
ACS Materials Lett. 2020, 2, 999−1007

electrode was able to attach on skin comfortably and successfully monitor vital electrophysiological signals (e.g., sEMG, EEG, and ECG). Moreover, the architecture of this skin-electrode was suitable for washable scenario and also that of repeated attaching-and-detaching-to-skin, meanwhile with comparable performance to commercial electrodes. To the best of our knowledge, our nestlike GFG is the first report of a nondisposable skin electrode for biometric signals based on monolayer graphene, revealing potential opportunities in wearable healthcare applications.

EXPERIMENTAL SECTION

Synthesis of GFG. A 1 cm × 2 cm copper foil was placed in the hot center of the furnace as the catalytic substrate. 200 sccm Ar was introduced into the system for ∼1 min to blow the air out. After being heated up to 1000 °C under an atmosphere of 20 sccm H_2 (1×10^{-1} Pa), the Cu foil continued to be heated for 60 min under the same condition. 35 sccm methane was introduced into the system and maintained for 30 min. Finally, methane gas supply was cut off and the sample was cooled to room temperature without changing the H_2 flow.

The nanofibers were electrostatically spun on the surface of graphene using 0.15 wt % mixed $CuCl_2$, SEBS, and PR in THF. In addition, the solution was loaded into a 2 mL syringe with a 26-gauge needle tip, which was connected to a voltage supply (Model DT-1005, Dalian DingTong Technology Co., Ltd.). A syringe pump (LEAD FLUID TYD01) was used to pump out solution. The pump rate, voltage, and needle-collector distance were 0.01 mL/h, 9 kV, and 10 cm, respectively, for electrospinning. The graphene film/Cu foil substrate was grounded to collect the electrospun nanofiber for a series of densities. Electrospun polymer/graphene film/Cu foil was next annealed at 600 °C for half an hour. Polystyrene-*block*-poly(ethylene-*ran*-butylene)-*block*-polystyrene (SEBS, MW ≈ 118 000, Aldrich) toluene solution (120 mg/mL) was dropcast on the annealed electrospun polymer/graphene film/Cu foil. The entire film was dried at room temperature for 4 h to evaporate toluene solvent. Finally, a stable and flexible GFG semi-embedded in SEBS was obtained by etching the copper foil in a $(NH_4)_2S_2O_8$ solution.

Characterization of GFG. The morphologies of the samples were observed using an optical microscope (Leica, Model DM2700 M) and SEM characterizations were done using a SEM (Hitachi, Model SU8010) with an acceleration voltage of 10 kV. The TEM and SAED images were collected using a TEM system (FEI Talos F200s, with an acceleration voltage of 300 kV). Elemental mapping was performed using a TEM equipped with an energy-dispersive X-ray spectroscopy (EDS) detector. The sheet resistance was measured with a four-probe Keithley Model 2636b Source Measure Unit. The Raman spectrum was measured on a spectrofluorometer (Edinburgh Instruments, Model FS5). The electrochemical impedance spectroscopy (EIS) measurements were conducted using an electrochemical workstation (Model CHI600e, CH Instruments, USA). The electrochemical impedance spectroscopy (EIS) measurements were conducted using an electrochemical workstation (Model CHI600e, CH Instruments, USA). A three-electrode configuration was used, with the potentials referenced to a $Hg/Hg_2Cl_2/KCl$ electrode, a platinum foil as counter electrode, and the GFG as working electrode. The measurements were performed in physiological saline at room temperature.

Electrophysiology Signal Detection. With regard to sEMG, two working electrodes were placed on the brachioradialis and one reference electrode was attached at the back of the hand. With regard to frontal cortex electrical signals monitoring, two electrodes were placed on the forehead with a ground patch electrode behind the ear. The subject is told to relax and try not to move his face while attempting to record EEGs; muscle movements can also be picked up, which causes interference with the EEG reading. EEG is one of the weaker electrophysiological signals, and it is important to remain still (do not move any muscle of the head) and reduce noise as much as possible. Conductive silver paste was used to connect the GFG electrodes to the copper wire, and when contacting the skin, insulating tape was applied to block the exposed part of the copper wire with the skin. Moreover, a 47-μm-thick stretchable medical tape (Tegaderm, 3M) was applied to provide a stable adhesion of electrodes to skin surface. sEMG, ECG, and EEG signals were amplified and pretreated by the commercialized device and software (Backyard Brains). In addition, the infrared images were obtained by using an thermal imager (UNI-T, Model UTi89).

ASSOCIATED CONTENT

Supporting Information

The supporting information is available. The Supporting Information is available free of charge at https://pubs.acs.org/doi/10.1021/acsmaterialslett.0c00203.

Additional figures for characterization of the fiber/graphene; schematic diagram of the GFG electrode; representative sEMG test results; and comparison of figure of merits (PDF)

AUTHOR INFORMATION

Corresponding Author

Nan Liu − *Beijing Key Laboratory of Energy Conversion and Storage Materials, College of Chemistry, Beijing Normal University, Beijing 100875, People's Republic of China; Beijing Graphene Institute, Beijing 100094, People's Republic of China;* orcid.org/0000-0002-1793-7372; Email: nanliu@bnu.edu.cn

Authors

Jiakang Qiu − *Beijing Key Laboratory of Energy Conversion and Storage Materials, College of Chemistry, Beijing Normal University, Beijing 100875, People's Republic of China; College of Physics Science & Information Engineering and Hebei Advanced Thin Film Laboratory, Hebei Normal University, Shijiazhuang, Hebei 050024, People's Republic of China*

Tianhao Yu − *Beijing Graphene Institute, Beijing 100094, People's Republic of China*

Weifeng Zhang − *Beijing Key Laboratory of Energy Conversion and Storage Materials, College of Chemistry, Beijing Normal University, Beijing 100875, People's Republic of China*

Zihan Zhao − *Beijing Key Laboratory of Energy Conversion and Storage Materials, College of Chemistry, Beijing Normal University, Beijing 100875, People's Republic of China*

Yan Zhang − *Beijing Key Laboratory of Energy Conversion and Storage Materials, College of Chemistry, Beijing Normal University, Beijing 100875, People's Republic of China*

Guo Ye − *Beijing Key Laboratory of Energy Conversion and Storage Materials, College of Chemistry, Beijing Normal University, Beijing 100875, People's Republic of China*

https://dx.doi.org/10.1021/acsmaterialslett.0c00203
ACS Materials Lett. 2020, 2, 999−1007

Yan Zhao − *Beijing Key Laboratory of Energy Conversion and Storage Materials, College of Chemistry, Beijing Normal University, Beijing 100875, People's Republic of China*
Xiaojia Du − *Beijing Key Laboratory of Energy Conversion and Storage Materials, College of Chemistry, Beijing Normal University, Beijing 100875, People's Republic of China*
Xu Liu − *Beijing Graphene Institute, Beijing 100094, People's Republic of China*
Lu Yang − *Beijing Graphene Institute, Beijing 100094, People's Republic of China*
Lijuan Zhang − *Beijing Graphene Institute, Beijing 100094, People's Republic of China*
Shuyan Qi − *Beijing Key Laboratory of Energy Conversion and Storage Materials, College of Chemistry, Beijing Normal University, Beijing 100875, People's Republic of China*
Qishuo Tan − *Beijing Key Laboratory of Energy Conversion and Storage Materials, College of Chemistry, Beijing Normal University, Beijing 100875, People's Republic of China*
Xinyu Guo − *Beijing Key Laboratory of Energy Conversion and Storage Materials, College of Chemistry, Beijing Normal University, Beijing 100875, People's Republic of China*
Guanmeng Li − *Beijing Key Laboratory of Energy Conversion and Storage Materials, College of Chemistry, Beijing Normal University, Beijing 100875, People's Republic of China*
Shaoshi Guo − *Beijing Key Laboratory of Energy Conversion and Storage Materials, College of Chemistry, Beijing Normal University, Beijing 100875, People's Republic of China*
Huiyuan Sun − *College of Physics Science & Information Engineering and Hebei Advanced Thin Film Laboratory, Hebei Normal University, Shijiazhuang, Hebei 050024, People's Republic of China;* orcid.org/0000-0001-8462-7609
Di Wei − *Beijing Graphene Institute, Beijing 100094, People's Republic of China*

Complete contact information is available at: https://pubs.acs.org/10.1021/acsmaterialslett.0c00203

Author Contributions

[▽]These authors contributed equally to this work.

Notes

The authors declare no competing financial interest.

■ ACKNOWLEDGMENTS

This work was financially supported by the Beijing Municipal Science & Technology Commission (No. Z191100000819002), National Natural Science Foundation of China (No. 21903007), Young Thousand Talents Program (No. 110532103), Beijing Normal University Startup funding (No. 312232102), and the Fundamental Research Funds for the Central University (No. 310421109).

■ REFERENCES

(1) Wang, S.; Xu, J.; Wang, W.; Wang, G.-J. N.; Rastak, R.; Molina-Lopez, F.; Chung, J. W.; Niu, S.; Feig, V. R.; Lopez, J.; Lei, T.; Kwon, S.-K.; Kim, Y.; Foudeh, A. M.; Ehrlich, A.; Gasperini, A.; Yun, Y.; Murmann, B.; Tok, J. B. H.; Bao, Z. Skin electronics from scalable fabrication of an intrinsically stretchable transistor array. *Nature* **2018**, *555*, 83−88.
(2) Chung, H. U.; Kim, B. H.; Lee, J. Y.; Lee, J.; Xie, Z.; Ibler, E. M.; Lee, K.; Banks, A.; Jeong, J. Y.; Kim, J.; et al. Binodal, wireless epidermal electronic systems with in-sensor analytics for neonatal intensive care. *Science* **2019**, *363*, No. eaau0780.
(3) Kim, D.-H.; Lu, N.; Ma, R.; Kim, Y.-S.; Kim, R.-H.; Wang, S.; Wu, J.; Won, S. M.; Tao, H.; Islam, A.; et al. Epidermal electronics. *Science* **2011**, *333*, 838−843.
(4) Wang, H.; He, M.; Zhang, Y. Carbon Nanotube Films: Preparation and Application in Flexible Electronics. *Wuli Huaxue Xuebao* **2019**, *35*, 1207−1223.
(5) Liu, Y.; Pharr, M.; Salvatore, G. A. Lab-on-Skin: A Review of Flexible and Stretchable Electronics for Wearable Health Monitoring. *ACS Nano* **2017**, *11*, 9614−9635.
(6) Norton, J. J. S.; Lee, D. S.; Lee, J. W.; Lee, W.; Kwon, O.; Won, P.; Jung, S.-Y.; Cheng, H.; Jeong, J.-W.; Akce, A.; Umunna, S.; Na, I.; Kwon, Y. H.; Wang, X.-Q.; Liu, Z.; Paik, U.; Huang, Y.; Bretl, T.; Yeo, W.-H.; Rogers, J. A. Soft, curved electrode systems capable of integration on the auricle as a persistent brain−computer interface. *Proc. Natl. Acad. Sci. U. S. A.* **2015**, *112*, 3920.
(7) Kwon, Y. H.; Fingert, J. H.; Kuehn, M. H.; Alward, W. L. Primary open-angle glaucoma. *N. Engl. J. Med.* **2009**, *360*, 1113−1124.
(8) Kabiri Ameri, S.; Ho, R.; Jang, H.; Tao, L.; Wang, Y.; Wang, L.; Schnyer, D. M.; Akinwande, D.; Lu, N. Graphene electronic tattoo sensors. *ACS Nano* **2017**, *11*, 7634−7641.
(9) Nawrocki, R. A.; Jin, H.; Lee, S.; Yokota, T.; Sekino, M.; Someya, T. Self-Adhesive and Ultra-Conformable, Sub-300 nm Dry Thin-Film Electrodes for Surface Monitoring of Biopotentials. *Adv. Funct. Mater.* **2018**, *28*, 1803279.
(10) Jeong, H.; Wang, L.; Ha, T.; Mitbander, R.; Yang, X.; Dai, Z.; Qiao, S.; Shen, L.; Sun, N.; Lu, N. Modular and Reconfigurable Wireless E-Tattoos for Personalized Sensing. *Adv. Mater. Technol.* **2019**, *4*, 1900117.
(11) Wang, Y.; Qiu, Y.; Ameri, S. K.; Jang, H.; Dai, Z.; Huang, Y.; Lu, N. Low-cost, μm-thick, tape-free electronic tattoo sensors with minimized motion and sweat artifacts. *npj Flexible Electron.* **2018**, *2*, 6.
(12) Liu, Z.; Wang, X.; Qi, D.; Xu, C.; Yu, J.; Liu, Y.; Jiang, Y.; Liedberg, B.; Chen, X. High-Adhesion Stretchable Electrodes Based on Nanopile Interlocking. *Adv. Mater.* **2017**, *29*, 1603382.
(13) Won, P.; Park, J. J.; Lee, T.; Ha, I.; Han, S.; Choi, M.; Lee, J.; Hong, S.; Cho, K.-J.; Ko, S. H. Stretchable and Transparent Kirigami Conductor of Nanowire Percolation Network for Electronic Skin Applications. *Nano Lett.* **2019**, *19*, 6087−6096.
(14) Yun, Y. J.; Ju, J.; Lee, J. H.; Moon, S. H.; Park, S. J.; Kim, Y. H.; Hong, W. G.; Ha, D. H.; Jang, H.; Lee, G. H.; et al. Highly Elastic Graphene-Based Electronics Toward Electronic Skin. *Adv. Funct. Mater.* **2017**, *27*, 1701513.
(15) Yeo, W. H.; Kim, Y. S.; Lee, J.; Ameen, A.; Shi, L.; Li, M.; Wang, S.; Ma, R.; Jin, S. H.; Kang, Z.; et al. Multifunctional epidermal electronics printed directly onto the skin. *Adv. Mater.* **2013**, *25*, 2773−2778.
(16) Fan, J. A.; Yeo, W.-H.; Su, Y.; Hattori, Y.; Lee, W.; Jung, S.-Y.; Zhang, Y.; Liu, Z.; Cheng, H.; Falgout, L.; et al. Fractal design concepts for stretchable electronics. *Nat. Commun.* **2014**, *5*, 3266.
(17) Choi, S.; Han, S. I.; Jung, D.; Hwang, H. J.; Lim, C.; Bae, S.; Park, O. K.; Tschabrunn, C. M.; Lee, M.; Bae, S. Y.; Yu, J. W.; Ryu, J. H.; Lee, S.-W.; Park, K.; Kang, P. M.; Lee, W. B.; Nezafat, R.; Hyeon, T.; Kim, D.-H. Highly conductive, stretchable and biocompatible Ag−Au core−sheath nanowire composite for wearable and implantable bioelectronics. *Nat. Nanotechnol.* **2018**, *13*, 1048−1056.
(18) Wu, W.; Haick, H. Materials and Wearable Devices for Autonomous Monitoring of Physiological Markers. *Adv. Mater.* **2018**, *30*, 1705024.
(19) Lyu, Q.; Zhai, Q.; Dyson, J.; Gong, S.; Zhao, Y.; Ling, Y.; Chandrasekaran, R.; Dong, D.; Cheng, W. Real-Time and In-Situ Monitoring of H2O2 Release from Living Cells by a Stretchable Electrochemical Biosensor Based on Vertically Aligned Gold Nanowires. *Anal. Chem.* **2019**, *91*, 13521−13527.
(20) Zhu, B.; Gong, S.; Cheng, W. Softening gold for elastronics. *Chem. Soc. Rev.* **2019**, *48*, 1668−1711.
(21) Yang, S.; Chen, Y. C.; Nicolini, L.; Pasupathy, P.; Sacks, J.; Su, B.; Yang, R.; Sanchez, D.; Chang, Y. F.; Wang, P.; et al. Cut-and-Paste" Manufacture of Multiparametric Epidermal Sensor Systems. *Adv. Mater.* **2015**, *27*, 6423−6430.

(22) Miyamoto, A.; Lee, S.; Cooray, N. F.; Lee, S.; Mori, M.; Matsuhisa, N.; Jin, H.; Yoda, L.; Yokota, T.; Itoh, A.; et al. Inflammation-free, gas-permeable, lightweight, stretchable on-skin electronics with nanomeshes. *Nat. Nanotechnol.* **2017**, *12*, 907−913.
(23) Shi, J.; Liu, S.; Zhang, L.; Yang, B.; Shu, L.; Yang, Y.; Ren, M.; Wang, Y.; Chen, J.; Chen, W. Smart Textile-Integrated Microelectronic Systems for Wearable Applications. *Adv. Mater.* **2020**, *32*, 1901958.
(24) Romero, F. J.; Castillo, E.; Rivadeneyra, A.; Toral-Lopez, A.; Becherer, M.; Ruiz, F. G.; Rodriguez, N.; Morales, D. P. Inexpensive and flexible nanographene-based electrodes for ubiquitous electrocardiogram monitoring. *npj Flexible Electron.* **2019**, *3*, 12.
(25) Jang, H.; Park, Y. J.; Chen, X.; Das, T.; Kim, M. S.; Ahn, J. H. Graphene-based flexible and stretchable electronics. *Adv. Mater.* **2016**, *28*, 4184−4202.
(26) Nair, R. R.; Blake, P.; Grigorenko, A. N.; Novoselov, K. S.; Booth, T. J.; Stauber, T.; Peres, N. M.; Geim, A. K. Fine structure constant defines visual transparency of graphene. *Science* **2008**, *320*, 1308−1308.
(27) Pinto, A. M.; Goncalves, I. C.; Magalhaes, F. D. Graphene-based materials biocompatibility: a review. *Colloids Surf., B* **2013**, *111*, 188−202.
(28) Miao, P.; Wang, J.; Zhang, C.; Sun, M.; Cheng, S.; Liu, H. Graphene Nanostructure-Based Tactile Sensors for Electronic Skin Applications. *Nano-Micro Lett.* **2019**, *11*, 71.
(29) Ren, H.; Zheng, L.; Wang, G.; Gao, X.; Tan, Z.; Shan, J.; Cui, L.; Li, K.; Jian, M.; Zhu, L.; Zhang, Y.; Peng, H.; Wei, D.; Liu, Z. Transfer-Medium-Free Nanofiber-Reinforced Graphene Film and Applications in Wearable Transparent Pressure Sensors. *ACS Nano* **2019**, *13*, 5541−5548.
(30) Yang, J. C.; Mun, J.; Kwon, S. Y.; Park, S.; Bao, Z.; Park, S. Electronic Skin: Recent Progress and Future Prospects for Skin-Attachable Devices for Health Monitoring, Robotics, and Prosthetics. *Adv. Mater.* **2019**, *31*, 1904765.
(31) Silva, B.; Correia, J.; Nunes, F.; Tavares, P.; Varum, H.; Pinto, J. Bird Nest Construction—Lessons for Building with Earth. *WSEAS Trans. Environ. Dev.* **2010**, *6*, 83−92.
(32) Jessel, H. R.; Chen, S.; Osovski, S.; Efroni, S.; Rittel, D.; Bachelet, I. Design principles of biologically fabricated avian nests. *Sci. Rep.* **2019**, *9*, 4792.
(33) Ren, H.; Zheng, L.; Wang, G.; Gao, X.; Tan, Z.; Shan, J.; Cui, L.; Li, K.; Jian, M.; Zhu, L. Transfer-Medium-Free Nanofiber-Reinforced Graphene Film and Applications in Wearable Transparent Pressure Sensors. *ACS Nano* **2019**, *13*, 5541.
(34) Liu, N.; Kim, K.; Hsu, P.-C.; Sokolov, A. N.; Yap, F. L.; Yuan, H.; Xie, Y.; Yan, H.; Cui, Y.; Hwang, H. Y.; Bao, Z. Large-scale production of graphene nanoribbons from electrospun polymers. *J. Am. Chem. Soc.* **2014**, *136*, 17284−17291.
(35) Lin, J.; Peng, Z.; Liu, Y.; Ruiz-Zepeda, F.; Ye, R.; Samuel, E. L. G.; Yacaman, M. J.; Yakobson, B. I.; Tour, J. M. Laser-induced porous graphene films from commercial polymers. *Nat. Commun.* **2014**, *5*, 5714.
(36) Chyan, Y.; Ye, R.; Li, Y.; Singh, S. P.; Arnusch, C. J.; Tour, J. M. Laser-Induced Graphene by Multiple Lasing: Toward Electronics on Cloth, Paper, and Food. *ACS Nano* **2018**, *12*, 2176−2183.
(37) Wang, H.; Wang, H.; Wang, Y.; Su, X.; Wang, C.; Zhang, M.; Jian, M.; Xia, K.; Liang, X.; Lu, H.; Li, S.; Zhang, Y. Laser Writing of Janus Graphene/Kevlar Textile for Intelligent Protective Clothing. *ACS Nano* **2020**, *14*, 3219−3226.
(38) Barakat, N. A.; Kanjwal, M. A.; Sheikh, F. A.; Kim, H. Y. Spider-net within the N6, PVA and PU electrospun nanofiber mats using salt addition: Novel strategy in the electrospinning process. *Polymer* **2009**, *50*, 4389−4396.
(39) Lu, N.; Kim, D.-H. Flexible and Stretchable Electronics Paving the Way for Soft Robotics. *Soft Robotics* **2014**, *1*, 53−62.
(40) Guo, C. F.; Sun, T.; Liu, Q.; Suo, Z.; Ren, Z. Highly stretchable and transparent nanomesh electrodes made by grain boundary lithography. *Nat. Commun.* **2014**, *5*, 3121.
(41) Liu, N.; Chortos, A.; Lei, T.; Jin, L.; Kim, T. R.; Bae, W.-G.; Zhu, C.; Wang, S.; Pfattner, R.; Chen, X.; et al. Ultratransparent and stretchable graphene electrodes. *Sci. Adv.* **2017**, *3*, No. e1700159.
(42) Fan, J. A.; Yeo, W. H.; Su, Y.; Hattori, Y.; Lee, W.; Jung, S. Y.; Zhang, Y.; Liu, Z.; Cheng, H.; Falgout, L.; Bajema, M.; Coleman, T.; Gregoire, D.; Larsen, R. J.; Huang, Y.; Rogers, J. A. Fractal design concepts for stretchable electronics. *Nat. Commun.* **2014**, *5*, 3266.
(43) Barold, S. S. Willem Einthoven and the birth of clinical electrocardiography a hundred years ago. *Card. Electrophysiol. Rev.* **2003**, *7*, 99−104.

https://dx.doi.org/10.1021/acsmaterialslett.0c00203
ACS Materials Lett. 2020, 2, 999−1007